

# Dynamical leaps due to microscopic changes in multilayer networks

MARINA DIAKONOVA<sup>1,2</sup>, JOSÉ J. RAMASCO<sup>2</sup> and VÍCTOR M. EGUÍLUZ<sup>2</sup>

<sup>1</sup> *School of Mathematical Sciences, Queen Mary University of London - London E1 4NS, UK*

<sup>2</sup> *Instituto de Física Interdisciplinar y Sistemas Complejos IFISC (CSIC-UIB), Campus UIB 07122 Palma de Mallorca, Spain*

received 20 December 2017; accepted 27 March 2017  
published online 13 April 2017

PACS 89.75.-k – Complex systems

PACS 89.75.Hc – Networks and genealogical trees

**Abstract** – Recent developments of the multilayer paradigm include efforts to understand the role played by the presence of several layers on the dynamics of processes running on the networks. The possible existence of new phenomena associated to the richer multilayer topology has been discussed and examples of these differences have been systematically searched for. Here, we show that the interconnectivity of the layers may have an important impact on the speed of the dynamics run in the network and that microscopic changes such as the addition of one single inter-layer link can notably affect the arrival at a global stationary state. As a practical testbed, these results obtained with spectral techniques are confirmed with a Kuramoto dynamics for which the synchronization consistently accelerates after the addition of single inter-layer links.

Copyright © EPLA, 2017

**Introduction.** – The ubiquity of processes naturally described by dynamics on networks raises important issues on the role played by network structure on the emergence of collective phenomena. It has been shown that spectral analysis of the associated adjacency and Laplacian matrices can offer insights into a variety of fundamental phenomena such as those relying upon spreading or diffusion mechanisms [1–3]. In particular, spectral methods are the basis to characterize synchronization and random walk diffusion in networks [4–7]. The second smallest eigenvalue  $\lambda_2$  is known to be related to the timescale to attain synchronization [8] and consensus [9], and its inverse is often interpreted as the “proper time” of the system to relax [10]. This quantity, which, depending on the literature, is known as “algebraic connectivity” or “spectral gap”, is also indicative of the time of diffusion [11]. While the role of  $\lambda_2$  in “simple” graphs is well understood, more effort is needed to characterize its role and behavior in more realistic (and therefore complex) contexts.

One such novel framework is that of a multilayer network [12–14]. Its usefulness extends from finance [15–17] and mobility [18,19], to epidemics [20,21] and societal dynamics [22–28]. The multilayer scenario is ostensibly non-trivial, in the sense that the phenomena observed on this system of interconnected networks cannot be straightforwardly reduced to an aggregate network [29].

The implication is that the multilayer structure plays a fundamental role in diffusive processes, and that, therefore, its effect on  $\lambda_2$  is a pertinent and open issue.

Diffusion on a multiplex, that is, a multilayer whose  $N$  nodes connect univocally across all layers, was considered in refs. [30,31]. By varying the inter-layer diffusion constant, these works found boundaries of  $\lambda_2$  for the multiplex in terms of the values for individual layers (see also [32]). For a general weighted two-layer multiplex with a varying inter-layer link weight  $p$ , these results were rephrased in terms of a structural transition [33]: it was found that below some critical  $p_c$ ,  $\lambda_2(p) \sim 2p$ , while for larger  $p$  the algebraic connectivity approaches an asymptote given by  $L_2 = \frac{1}{2}\lambda_2(\mathcal{L}_1 + \mathcal{L}_2)$ , where  $\mathcal{L}_{1,2}$  are the Laplacian matrices of the two layers and  $\lambda_2(\mathcal{L}_1 + \mathcal{L}_2)$  refers to the spectral gap of the multilayer network. The changing character of the functional growth of  $\lambda_2$  suggests the existence of two regimes, an “underconnected” one with the two layers functioning autonomously, and a “multiplex” one where the inter-layer connectivity plays the dominant role. It has been noted that the presence of the point of inflection  $p_c$  might follow from linear algebra arguments [34], and, depending on the topology of the inlayer networks,  $p_c$  may tend to zero in the limit of  $N \rightarrow \infty$  [35]. It is still under study how significant this change is in describing the observed changes in the dynamic timescales [36].

This work extends the analysis of multiplex timescales to cover the effect of the specific type of inter-layer coupling. Instead of gradually tuning up the intensity of inter-layer links  $p$ , we now switch on the inter-layer links at unit intensity one by one. Our strategy of considering binary weight on the inter-layer links corresponds to a natural situation where these links are either absent or present, and where one can preferentially control the amount, and the placement, of such links. Note that this changes the framework, which passes from multiplex to more general multilayer networks. Spectral properties resulting from such inter-layer link sequences, and their placement, were considered in [10]. The authors studied identical partially coupled networks, and found that the trends of average algebraic connectivity showed a qualitative change at an (analytically derivable) minimum number of inter-layer links, depending on the placement of their end points. The authors of [37] elucidated the optimal relation between the similarity of layers and the weight of inter-layer links, given some minimization constraint. Here we consider non-identical, general layers (see ref. [38] for the study of a multiplex with widely different inter-layer structure), and instead focus on the effect of the addition of inter-layer links to individual systems. We find that  $\lambda_2(q)$  of the fraction  $q$  of such an inter-layer connection sequence is characterized by leaps, implying sudden decreases in the timescales of the resulting multilayer. We characterize the statistics of these jumps and elucidate the way in which the layer degree correlation [39,40] affects them. Our results show that not only are highly correlated multilayers connected with high intensities on average slower than anti-correlated multilayer networks, but that the statistics of jumps are qualitatively different for distinct types of ordering. Finally, we validate our findings by running Kuramoto dynamics on the multilayers, and verifying that  $\lambda_2$  does indeed inform on the scaling of the approach to the fully synchronized state.

**Multilayer networks.** – The first step is to describe how the networks used in the analysis are built. Inspired by the construction of multiplexes, we consider multilayers formed of statistically equivalent networks with the same number of nodes  $N$  on each layer. For simplicity, the networks are formed of only two layers  $G_1$  and  $G_2$ , which along with the inter-layer connections constitute the multilayer  $G$ . In each of the layers, the network is built using a Molloy-Reed configurational algorithm with  $\gamma = 2.5$  [41] and a weight of unity on each intra-layer link. The inter-layer edges connect a fraction  $q$  of the  $N$  nodes of the two layers with an intensity  $p$ . Three procedures to draw inter-layer connections are considered depending on the inlayer number of connection of the nodes (degree) (see fig. 1). The first one is simply uncorrelated (UnC) regardless of the nodes inlayer degrees. This is the baseline scenario and has been profusely used in the literature. The other two procedures include some correlation between the degrees of the nodes connected across layers.

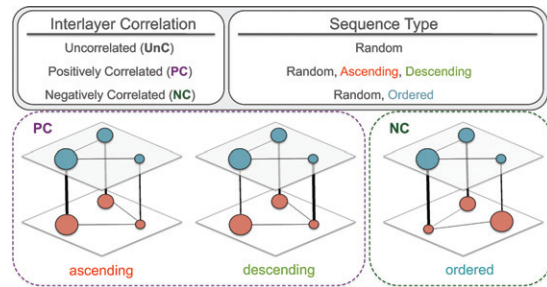


Fig. 1: (Color online) Some connection sequence schema for a positively correlated and a negatively correlated multilayer.

The positively correlated (PC) method preferentially connects high-degree nodes in one layer  $G_1$  with their counterparts in the other layer  $G_2$ . Conversely, the negatively correlated (NC) procedure establishes links between high-degree nodes in  $G_1$  and low-degree nodes in  $G_2$  and vice versa. Within the different categories of correlations, the inter-layer links can be drawn at random or following some order based on the nodes inlayer degrees. The possible sequence types corresponding to each layer correlation are shown in fig. 1. For a PC multilayer, an ascending sequence connects node pairs starting from those that have the lowest degree, the descending sequence starts from the node pairs with the highest degree. In a NC multilayer the ordered sequence establishes connections between high-degree nodes on one layer and the low-degree nodes in another first. Thus, to create a multilayer  $M(p, q)$  we must specify: a) the size  $N$  of each layer, b) the layer correlation strategy (UnC, PC or NC), c) the strength of inter-layer connections  $p$  and the fraction of connected nodes  $q$ , and d) the sequence type that gives the order in which layers become interconnected.

**Building the supra-Laplacian.** – For each realization of  $M(p, q)$ , we compute the algebraic connectivity  $\lambda_2$  of the supra-Laplacian  $\mathcal{L}$ . The procedure for constructing the supra-Laplacian of a multiplex with  $q = 1$  is detailed in [33], yielding

$$\mathcal{L} = \begin{pmatrix} \mathcal{L}_1 + p\mathbb{1} & -p\mathbb{1} \\ -p\mathbb{1} & \mathcal{L}_2 + p\mathbb{1} \end{pmatrix}, \quad (1)$$

where  $\mathcal{L}_k$  stands for the Laplacian of the layer  $G_k$ , separately, and  $\mathbb{1}$  is the unit  $N \times N$  matrix. In order to generalize the formalism to a situation in which some nodes are not connected across layers ( $q \neq 1$ ), we assign to such nodes, *e.g.*, node  $i$  in  $G_1$ , a partner down in  $G_2$  (arbitrarily, the node with the same index  $i$ ), but set the corresponding inter-layer link intensity equal to zero,  $p_i = 0$ . Thus, a multilayer  $M(p, q)$  will have a supra-Laplacian where the elements in the matrices  $p\mathbb{1}$  corresponding to positions  $i$  are zero instead of  $p$ .

**Initial results.** – The behavior of  $\lambda_2$  for different multilayer structures  $M(p, q)$  is shown in fig. 2 as a function of the inter-layer link intensity  $p$ . In fig. 2(a), the multilayer

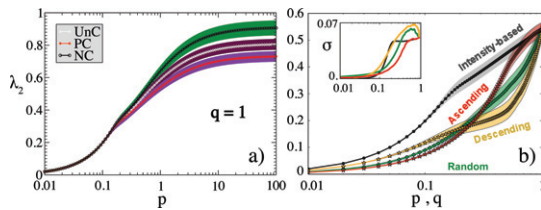


Fig. 2: (Color online)  $\lambda_2$  for a  $N = 100$  scale-free multilayers. (a) Mean and standard deviation over realizations (shaded region) of  $\lambda_2$  of  $M(p, q = 1)$  as a function of  $p$  with positive (PC), negative (NC), and neutral (UnC) inter-layer correlations, for 100 realizations. (b) Average  $\lambda_2$  for the PC case of (a) (labelled “intensity-based”) as a function of  $q$  for multilayers  $M(p = 1, q)$  with PC layers and three different connection sequences, all for  $10^3$  realizations. Inset: standard deviation of the respective curves across the realizations.

is complete ( $q = 1$  so the network is a multiplex) and the results of [33] are recovered. The algebraic connectivity displays an inflection point for a particular value of  $p$ ,  $p_x$ , around 0.2 regardless of the correlations between the degrees of the nodes in both layers. This point marks the beginning of a different type of dynamics, passing from a single-layer driving one for  $p < p_x$  to an integrated network one for larger  $p$ . The correlations do play a role in the second integrated regime where they influence the relaxation time of the system (slower for PC and faster for NC with respect to the uncorrelated baseline). Increasing the system size  $N$  only magnifies these differences. Interestingly, after the inflection point the fluctuations in  $\lambda_2$  between realizations of the multilayer increase and remain constant with increasing  $p$ . The particular position of  $p_x$  displays a dependence on the system size in the range explored here numerically, but the presence of this regime of high  $\lambda_2$  variability across realizations always appears. It is worth noting as well that in contrast to ordinary phase transitions the increase in  $\sigma$  is not constrained to the neighborhood of  $p_x$ .

If the intensity of the inter-layer connections is kept constant,  $p = 1$ , and  $q$  is varied instead, these curves notably change and their shape depends on the particular order implemented in the inter-layer node connection to build the multilayer (see fig. 2(b)).  $\lambda_2$  is lower for a multilayer network with fewer inter-layer links (with heavier weight of unity) than for a multiplex with fully interconnected layers but at small intensities. That is to some extent intuitive, as the missing inter-layer connections might have been much more necessary for the “emergent” multilayer, and having them present albeit at a small intensity would connect the layer more strongly. In addition, the three possible sequences behave differently depending on  $q$ . For small  $q$ , until about  $q < q = p_x$ , they increase linearly with  $q$ . The descending sequence results in a consistently greater  $\lambda_2$ , implying a faster dynamics on the multilayer (this seems to be a generic result [42]). This is manifestly not the case at high  $q$  where the situation reverses. Besides the

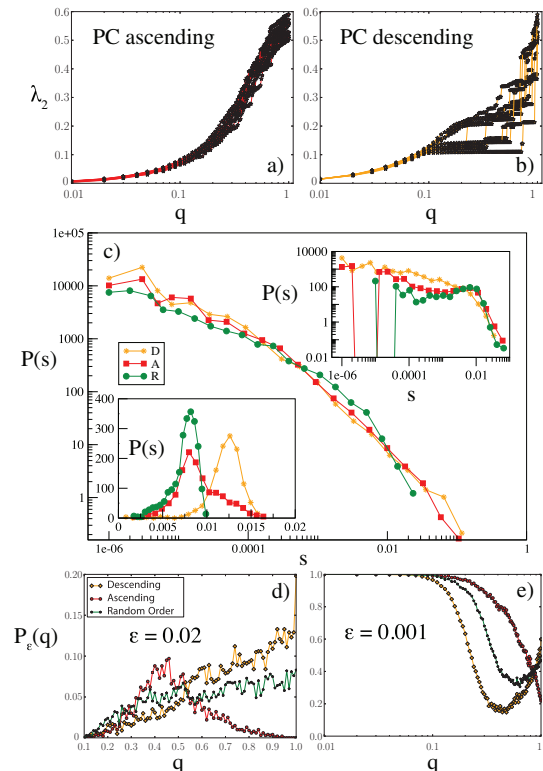


Fig. 3: (Color online) Partial connectivity sequences in positively correlated scale-free multilayers with  $N = 100$ ,  $p = 1$ . (a) and (b):  $\lambda_2$  as a function of  $q$  for the ascending and descending degree sequences. The plots contain ten realization in total although the curves are displayed realization by realization. (c) Probability density distribution of the differences between consecutive values of  $\lambda_2$  as a new link is introduced for the three different sequence types D (descending), A (ascending) and R (random), computed over  $10^3$  realizations at  $q = 0.9$  (main plot),  $q = 0.2$  (top right inset) and  $q = 0.05$  (bottom left inset). The main plot and right inset are in log-log scale, the left inset is in linear scale. (d) and (e): probability  $P_\epsilon$  to see jumps higher than  $\epsilon$ , computed at each  $q$  value over 1000 realizations, for each of the ascending, descending and neutral sequences.

average  $\lambda_2$ ,  $\sigma$  displays a similar behavior as in the case of  $q = 1$ : beyond  $p_x$  it increases and remains high afterward, although with peculiarities due to the sequence and correlations of the inter-layer connections (see inset of fig. 2(b)).

**Leaps in the largest eigenvalue.** – On single network realizations instead of on average properties, we find what is the most important result of this work. The multilayer  $M(p = 1, q)$  from the previous section is constructed by adding inter-layer links of unit weight one by one until their fraction is equal to  $q$ . This process accumulates microscopic changes to end up in a macroscopic configuration of the multilayer networks. Naively, one could expect one of such microscopic changes to be innocuous to the macroscopic picture and, consequently, to have a very minor impact on the dynamics of any process taking place on the multilayer. However, this expectation is wrong as can

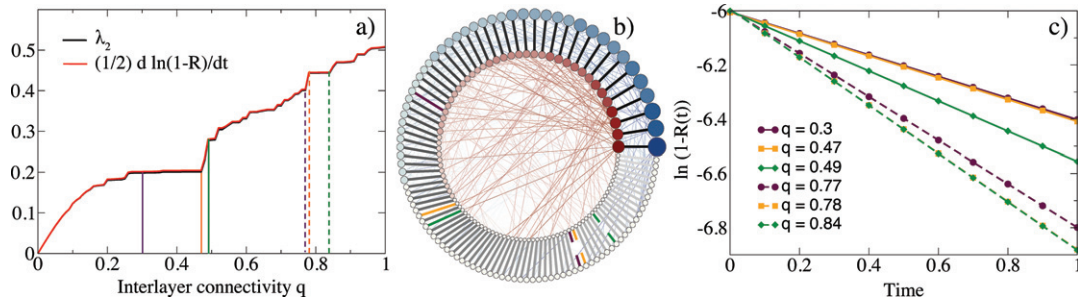


Fig. 4: (Color online) Validation of the effects of the  $\lambda_2$  jumps on the timescales of processes running on a PC multilayer  $M(p = 1, q)$  with  $N = 100$  generated with a sequence descending in degree. (a)  $\lambda_2$  and the numeric derivative of  $\ln(1 - R(t))$  as a function of  $q$ . (b) A graphical representation of the multilayer  $M(p = 1, q^*)$  in concentric circles, with nodes arranged counterclockwise and their size and location proportional to their degree, where  $q^*$  is from the set of lines in panel (a) with the corresponding colors. (c) The temporal relaxation of the order parameter  $\ln(1 - R(t))$  for each  $q^*$ .

be seen in fig. 3(a) and (b) on an example with a positively correlated multilayer. The value of  $\lambda_2$  experiences significant jumps after the introduction of a single link across layers. The smooth behavior characteristic of the absence of jumps in  $\lambda_2$  is only visible in a sparsely interconnected multilayers (lower  $q$ ), where for some range (but depending on the sequence) the increase is linear,  $\lambda_2(q) \propto q$ . Although the frequency and location of  $\lambda_2(q)$  discontinuities depend on the specific realization, on average they occur at some large  $q$ . Since  $\lambda_2$  is a global feature of the multilayer, the “offending” link is intrinsically connected to some global property of the layers, or to the sequences themselves. We have checked whether this relates to the betweenness of the new added link, but the results are not positive. Such sudden leaps reflect the precarious nature of adding final inter-layer connections, implying that after some minimal number of connections has been set, it becomes very hard to predict the exact effect of the addition of each inter-layer link.

The distribution of jumps is included in fig. 3(c), where beyond the sequence the width of the distribution is controlled by the final value of  $q$ . Varying this parameter, one can observe long tailed distributions in the changes of  $\lambda_2$  spanning several orders of magnitude as in the main plot or in the top-right inset, or more constrained jump distributions as those of the left-bottom inset for smaller values of  $q$ . For most of the values of  $q$ , the dominating effect is the non-trivial long-tailed distributions. To explore this further, we introduce a cutoff  $\epsilon$  and measure the probability  $P_\epsilon(q)$  to have an increase in  $\lambda_2$  by at least  $\epsilon$  at the addition of the subsequent link. At intermediate  $\epsilon$  values (fig. 3(d)), it identifies that the main difference between the ascending and the descending sequence is not that the former has fewer jumps (which could have been expected from the lower standard deviation), but that the jumps are centered at some  $q$ , with a well-defined mean. The descending sequence and the random one, on the other hand, show a completely different profile of a monotonically increasing jump probability. If the last node pairs to be interconnected are those with the lowest degrees, their addition is much more likely to cause a sudden jump in

the speeds of the diffusion, than if the last interconnected nodes had high degree. That, however, is because in the latter case the multilayer would already have been relatively fast. The reason lies in another curious observation shown in fig. 3(e). The probability of *at least a minute jump* is minimized at some  $q < 1$  for the descending and random sequences, and decreases monotonically for the ascending one. This lack of change is difficult to achieve if lower-degree nodes were interconnected first.

**Validation.** – Calculating  $\lambda_2$  implies non-linear operations and one might wonder if these results were not an artifact of the numerical methods. To verify their relevance for dynamical processes occurring on the multilayers, we run the Kuramoto model and compare the variations in  $\lambda_2$  with the synchronization timescales. Specifically, an oscillator is placed in each node  $i$  of the multilayer with phase  $\theta_i$ . The oscillators have the same natural frequency and the evolution of their phases is described after linearization by the following equation [43,44]:

$$\dot{\theta}_j = \sum_{k \neq j} W_{jk} (\theta_k - \theta_j), \quad (2)$$

where  $W_{jk}$  are the elements of the adjacency matrix with the corresponding weights for intra- and inter-layer links. To ensure an easier measurement of the timescales, the initial state of the system is set at the value of the eigenvector associated with  $\lambda_2$ . Under these conditions, the system approaches synchronization as

$$1 - R(t) \propto e^{-2\lambda_2 t}, \quad (3)$$

where  $R$  is the phase coherence of the population,  $R = |\sum_j e^{i\theta_j}|$ , and plays the order parameter in the synchronization transition.

In fig. 4, we show how the changes in the spectral gap  $\lambda_2$  actually translates to changes in the relaxation times. In fig. 4(a),  $\lambda_2$  and the inverse relaxation times are displayed as a function of  $q$  for a PC multilayer built in descending degree sequence. Both coincide as it must be if the numeric estimation of  $\lambda_2$  is appropriate. Several jumps

can be observed and are marked with vertical lines of different colors and textures. These changes occur after the introduction of single links as represented in fig. 4(b). The presence of these single links brings about an important variation in the macroscopic system relaxation as can be seen in fig. 4(c). The underlying exponential decays for a selected range of  $q$  values chosen to lie around two significant jumps. The observed straight lines imply that  $\alpha$  is well defined as an exponent even in the vicinity of the jumps, and hence that the decrease in timescales is indeed abrupt.

**Conclusions.** – Our results thus show that the jumps in the algebraic connectivity are not merely a numeric artifact, but instead correspond to the measured abrupt decreases in the synchronization timescales of the dynamical system. This ratifies that microscopic changes in the topological properties of these multilayer networks lead to effects noticed at a global scale. We also investigated the characteristics of these offending node pairs whose interconnection causes the jumps, but did not detect any special local or simple global network feature. The lack of any correspondence between the degree, and the degree of the neighbors, of the selected nodes points to the non-trivial nature of the connection between the network properties of the multilayer nodes and their role as crucial mediators in enhancing the synchronization time of the multilayer, and calls for the use of global spectral methods to determine their location and quantify the possible effects of their introduction or deletion.

\* \* \*

Partial financial support has been received from the Spanish Ministry of Economy (MINECO) and FEDER (EU) under the project ESOTECOS (FIS2015-63628-C2-2-R), from the EPSRC project GALE, EP/K020633/1 and from the EU Commission through project LASAGNE (318132).

## REFERENCES

- [1] BOGUÑA M., PASTOR-SATORRAS R. and VESPIGNANI A., in *Statistical Mechanics of Complex Networks*, edited by PASTOR-SATORRAS R., RUBI M. and DÍAZ-GUILERA A., in *Lect. Notes Phys.*, Vol. **625** (Springer, Heidelberg) 2003, pp. 127–147.
- [2] JAMAKOVIC A., KOOLJ R., VAN MIEGHEM P. and VAN DAM E., *Robustness of networks against the spread of viruses: the role of the spectral radius*, in *Proceedings of the 13th Annual Symposium on Communications and Vehicular Technology in the Benelux (Liege, Belgium) 2006* (IEEE) 2006, doi: 10.1109/SCVT.2006.334367, pp. 35–38.
- [3] DOROGOVTSSEV S. N., GOLTSEV A. V. and MENDES J. F. F., *Rev. Mod. Phys.*, **80** (2008) 1275.
- [4] ATAY F. M., BITIKOGLU T. and JOST J., *Physica D: Nonlinear Phenom.*, **224** (2006) 35.
- [5] ARENAS A., DÍAZ-GUILERA A. and PÉREZ-VICENTE C. J., *Physica D: Nonlinear Phenom.*, **224** (2006) 27.
- [6] GÓMEZ-GARDEÑES J., MORENO Y. and ARENAS A., *Phys. Rev. Lett.*, **98** (2007) 034101.
- [7] CHEN J., LU J. A., ZHAN C. and CHEN G., *Laplacian spectra and synchronization processes on complex networks*, in *Handbook of Optimization in Complex Networks*, edited by THAI M. T. and PARDALOS P. M., *Springer Optimization and Its Applications*, Vol. **57** (Springer) 2012, pp. 81–113.
- [8] ALMENDRAL J. A. and DÍAZ-GUILERA A., *New J. Phys.*, **9** (2007) 187.
- [9] ESTRADA E., VARGAS-ESTRADA E. and ANDO H., *Phys. Rev. E*, **92** (2015) 052809.
- [10] MARTÍN-HERNÁNDEZ J., WANG H., VAN MIEGHEM P. and D’AGOSTINO G., *Physica A: Stat. Mech. Appl.*, **404** (2014) 92.
- [11] LOVÁSZ L., Technical Report YALEU/DCS/TR-1029, Department of Computer Science, Yale University, 1994.
- [12] BOCCALETTI S., BIANCONI G., CRIADO R., DEL GENIO C., GÓMEZ-GARDEÑES J., SENDIÑA-NADAL I., WANG Z. and ZANIN M., *Phys. Rep.*, **544** (2014) 1.
- [13] KIVELÄ M., ARENAS A., BARTHELEMY M., GLEESON J. P., MORENO Y. and PORTER M. A., *J. Complex Netw.*, **3** (2014) 203.
- [14] LEE K. M., MIN B. and GOH K. I., *Eur. Phys. J. B*, **88** (2015) 1.
- [15] DI IASIO G., BATTISTON S., INFANTE L. and PIEROBON F., in *Munich Personal RePEc Archive*, paper 52141, available at <https://mpra.ub.uni-muenchen.de/52141> (2013).
- [16] POLEDNA S., MOLINA-BORBOA J. L., MARTÍNEZ-JARAMILLO S., VAN DER LEIJ M. and THURNER S., *J. Financ. Stab.*, **20** (2015) 70.
- [17] BURKHOLZ R., LEDUC M. V., GARAS A. and SCHWEITZER F., *Physica D: Nonlinear Phenom.*, **323-324** (2016) 64.
- [18] DE DOMENICO M., SOLÉ-RIBALTA A., GÓMEZ S. and ARENAS A., *Proc. Natl. Acad. Sci. U.S.A.*, **111** (2014) 8351.
- [19] STRANO E., SHAI S., DOBSON S. and BARTHELEMY M., *J. R. Soc. Interface*, **12** (2015) 20150651.
- [20] GRANELL C., GÓMEZ S. and ARENAS A., *Phys. Rev. Lett.*, **111** (2015) 128701.
- [21] VAZQUEZ F., SERRANO M. A. and SAN MIGUEL M., *Sci. Rep.*, **6** (2016) 29342.
- [22] MUCHA P. J., RICHARDSON T., MACON K., PORTER M. A. and ONNELA J. P., *Science*, **328** (2010) 876.
- [23] BULDYREV S. V., PARSHANI R., PAUL G., STANLEY H. E. and HAVLIN S., *Nature*, **464** (2010) 1025.
- [24] KLIMEK P. and THURNER S., *New J. Phys.*, **15** (2013) 063008.
- [25] CSERMELY P., *Talent Dev. Excell.*, **5** (2013) 115.
- [26] WANG Z. and PERC A. S. M., *Sci. Rep.*, **3** (2013) 2470.
- [27] DIAKONOVA M., SAN MIGUEL M. and EGUÍLIZ V. M., *Phys. Rev. E*, **89** (2014) 062818.
- [28] KLIMEK P., DIAKONOVA M., EGUÍLIZ V. M., SAN MIGUEL M. and THURNER S., *New J. Phys.*, **18** (2016) 083045.
- [29] DIAKONOVA M., NICOSIA V., LATORA V. and SAN MIGUEL M., *New J. Phys.*, **18** (2016) 023010.
- [30] GÓMEZ S., DÍAZ-GUILERA A., GÓMEZ-GARDEÑES J., PÉREZ-VICENTE C. J., MORENO Y. and ARENAS A., *Phys. Rev. Lett.*, **110** (2013) 028701.

- [31] SOLÉ-RIBALTA A., DE DOMENICO M., KOUVARIS N. E., DÍAZ-GUILERA A., GÓMEZ S. and ARENAS A., *Phys. Rev. E*, **88** (2013) 032807.
- [32] DARABI SAHNEH F., SCOGLIO C. and VAN MIEGHEM P., *Phys. Rev. E*, **92** (2015) 040801.
- [33] RADICCHI F. and ARENAS A., *Nat. Phys.*, **9** (2013) 717.
- [34] GARRAHAN J. P. and LESANOVSKY I., available at <http://arxiv.org/abs/arXiv:1406.4706> (2014).
- [35] SAHNEH F. D., SCOGLIO C. and VAN MIEGHEM P., *Phys. Rev. E*, **92** (2015) 040801.
- [36] BASTAS N., LAZARIDIS F., ARGYRAKIS P. and MARAGAKIS M., *EPL*, **109** (2015) 38006.
- [37] SHAKERI H., ALBIN N., DARABI SAHNEH F., POGGI-CORRADINI P. and SCOGLIO C., *Phys. Rev. E*, **93** (2016) 030301.
- [38] GAMBUZZA L. V., FRASCA M. and GÓMEZ-GARDEÑES J., *EPL*, **110** (2015) 20010.
- [39] RADICCHI F., *Phys. Rev. X*, **4** (2014) 021014.
- [40] NICOSIA V. and LATORA V., *Phys. Rev. E*, **92** (2015) 032805.
- [41] MOLLOY M. and REED B., *Random Struct. Algorithms*, **6** (1995) 161.
- [42] AGUIRRE J., SEVILLA-ESCOBOZA R., GUTIÉRREZ R., PAPO D. and BULDÚ J. M., *Phys. Rev. Lett.*, **112** (2014) 248701.
- [43] KURAMOTO Y., *Chemical Oscillations, Waves, and Turbulence* (Springer-Verlag, New York) 1984.
- [44] ARENAS A., DÍAZ-GUILERA A., KURTHS J., MORENO Y. and ZHOU C., *Phys. Rep.*, **469** (2008) 93.